

Interactions of NO_2^- and SO_3^{2-} with Organic Triplets. Charge Transfer versus Energy Transfer: The Role of Reorganization Energy in Triplet-Anion Interactions and Spectroscopic Methods for Its Evaluation

I. Loeff, A. Treinin,*

Department of Physical Chemistry and the Farkas Center for Light-Induced Processes, Hebrew University, Jerusalem, 91904 Israel

and H. Linschitz*

*Department of Chemistry, Brandeis University, Waltham, Massachusetts 02254-9110
(Received: October 23, 1991; In Final Form: March 16, 1992)*

Charge-transfer (CT) and energy-transfer (NT) interactions of simple anions with organic triplets are reviewed and discussed in connection with new quenching rate constant (k_q) and radical yield measurements for SO_3^{2-} and NO_2^- . In the latter case, both processes may occur at high organic triplet energies. Reorganization energies for one-electron oxidations are obtained for several anions, using data on charge-transfer-to-solvent (CTTS) spectra and photoelectron emission thresholds, which, like the kinetic parameters of Marcus-Hush theory, also reflect Franck-Condon strains. These results, combined with thermodynamic free energies, give vertical redox potentials which correlate better than do equilibrium potentials with quenching rates. The theoretical basis for correlation between k_q and $h\nu_{\text{CTTS}}$ is discussed in the framework of Marcus rate theory. Assigning the total reorganization energy in the CT quenching reaction to the small anion component of the D-A pair gives reasonable agreement with data on quenching of dye triplets but too slow rates for aryl carbonyl triplets where exciplex formation may possibly occur. The optical reorganization energy for NO_2^- leads to values of the thermal self-exchange rate agreeing with those computed from the Marcus-Hush cross-relations, which also neglect bonding effects. The mechanism of NO_2^- interaction with triplets is discussed in detail, including indirect kinetic evidence for quenching of a short-lived exciplex by NO_2^- without radical formation. The possibility of reduction by triplet NO_2^- formed by initial NT from the organic triplet is also considered. Finally, a scheme is presented involving an equilibrium between CT and NT states and relating the free energy difference between these states to radical yields.

Introduction

Competitive quenching of excited molecules by concurrent charge-transfer and energy-transfer pathways and its effect on radical yield is a subject of interest from both theoretical and practical points of view. However, most quenching studies have been confined to systems where only one pathway was assumed to prevail (an assumption usually made "without adequate evidence"¹). Moreover, even in those studies which were mainly concerned with this problem (ref 1 and other references included therein), the factors determining the relative rates and efficiencies of the two processes have not been well established. The energy factor, including bond and solvent reorganization barriers, has been considered^{1,2} but with limited experimental results to support the ensuing conclusions.

Our studies on the interaction of simple inorganic anions with various organic triplets have shown that this leads to radical formation *accompanying* triplet removal only with certain anions ("group II").³⁻⁵ This group includes SO_3^{2-} , NO_2^- , HCO_2^- , and, to a lesser degree, N_3^- . The absence of radical formation for other simple anions ("group I", including halides, SCN^-) was attributed to strong spin-orbit coupling within the triplet-quencher complex, favoring rapid transition to the ground state.^{3,4} However, the radical yield with NO_2^- depended sharply on the thermodynamic properties of the triplet.³ Since the triplet energy of NO_2^- is low (2.3 eV),^{6,7} the possibility was considered³ of quenching by energy transfer (NT) in competition with charge transfer (CT).

We now report new studies on the interaction of NO_2^- and SO_3^{2-} (and other ions for comparison) with various triplets and consider these data in the general context of CT interactions of simple anions with excited large aromatic molecules. From the standpoint of current theories of electron transfer⁸⁻¹⁰ these systems permit physically reasonable simplifications to be made, in particular, to assign most of the reorganization free energy barrier to the small anion component of a charge-transfer pair. Methods to evaluate these barriers are described, using data on related electron-transfer phenomena which also involve Franck-Condon

strains, namely, charge-transfer-to-solvent (CTTS) spectra¹¹ and photoemission energy thresholds.¹² Resulting correlations between rates of CT quenching and $h\nu_{\text{CTTS}}$ are discussed. The view that NT predominates in some cases of NO_2^- quenching is reinforced by the appearance of low activation barriers in the process. We propose that the dominant quenching mechanism in a given case, when both are energetically feasible, will be the most exoergic reaction pathway available to the system.

Experimental Section

Materials. Sodium anthraquinone-2-sulfonate (AQS), 1,4-naphthoquinone (NQ), and xanthone were all of puriss. grade (Fluka) and were used as received. Benzophenone-4-carboxylic acid (BC, Aldrich) was recrystallized twice from ethanol. Sodium benzophenone-4-sulfonate (BS) was prepared by the method of Ramsey and Cohen¹³ and was recrystallized three times from ethanol. Eosin Y (Fluka) was purified chromatographically on an activated aluminum oxide column, precipitated by addition of 0.1 M HCl, and dried at 60 °C.

Acetonitrile (Burdick and Jackson) was glass distilled. All the inorganic materials used were of AnalaR quality. Water was purified by a Millipore-Q system.

Solutions were deaerated or oxygenated (1 atm of O_2) by bubbling N_2 or O_2 , respectively. Studies of BC and BS were carried out at pH 11.2 (adjusted by NaOH) as in earlier work⁵ to put the ketyl radicals completely into the anionic form ($\text{p}K_a$ - (BCH) = 8.2). Xanthone and eosin were also studied in alkaline solutions (10^{-2} M NaOH and 10^{-2} M borax, pH 9.1, respectively), and 16% (v/v) CH_3CN was added to the xanthone solutions to increase its solubility. Separate solutions of carbonyl compound and quencher were mixed shortly before use to minimize thermal reactions. Absorption spectrum measurements gave no indication of ground-state interactions in any of the systems studied, except for xanthone- SO_3^{2-} , where only dilute Na_2SO_3 solutions (below 2×10^{-2} M) could be used. NQ-SO_3^{2-} solutions were too unstable to be studied.

Apparatus and Procedure. Except for eosin, the carbonyl compounds were excited at 337.1 nm by a pulsed nitrogen laser (P.R.A. LN-1000, 0.5 ns, 1.5 mJ). Kinetic traces were digitized and amplified by either a Tektronix 2430 or 7912 oscilloscope, according to their lifetimes. An Olivetti PC was used for averaging and storing data. The other components were conventional, including a pulsed xenon lamp, monochromator, and fast photomultiplier, with collinear measuring and excitation beams. Eosin was excited at 480 nm with a dye laser (Molelectron DL-200, coumarin 481 in dioxane, pumped by a UV-14 nitrogen laser). The fwhm of the two lasers is about 10 ns.

The concentration of the carbonyl compound was usually adjusted to give absorbance ~ 1 at 337 nm, and that of NO_2^- was kept low to minimize its light absorption. This precaution was unnecessary in the eosin case, since NO_2^- does not absorb at 480 nm. In some of these systems the rate of triplet decay depends on ground-state concentration (T + G interactions), and therefore these concentrations were kept constant (photoconversions were low) throughout the whole set of experiments designed to measure quenching rate constants. However, this effect should be considered when comparison is made with any earlier data.

Quenching Rate Constants. Second-order rate constants, k_q , for quenching of triplets by the inorganic anions were usually obtained from the linear dependence of pseudo-first-order triplet decay constants on anion concentration, following the triplet absorption near its peak. In some cases, where there were overlapping transient absorptions, the decay of the triplet or the growth of the reduced species was followed at other wavelengths. Such was the case for $\text{BC} + \text{SO}_3^{2-}$ where measurements of the triplet decay at 410 nm (λ_{max} of triplet, 535 nm) and the growth of the ketyl anion at 660 nm gave closely agreeing results: $k_q = (3.5 \pm 0.5) \times 10^8 \text{ M}^{-1} \text{ s}^{-1}$. An indirect method involving competitive quenching was also used:⁵ the absorbance D of BC^- was measured at constant $[\text{SO}_3^{2-}]$, ensuring total quenching, with various concentrations of Br^- , which quenches (below 0.1 M) without radical formation.¹⁴ From a plot of D^0/D (D^0 is M^- absorbance at $[\text{Br}^-] = 0$) against $[\text{Br}^-]$ and knowing the value of $k_q^{\text{Br}^-} = 2.2 \times 10^8 \text{ M}^{-1} \text{ s}^{-1}$, the quenching constant $k_q^{\text{SO}_3^{2-}} = 3.0 \times 10^8 \text{ M}^{-1} \text{ s}^{-1}$ was obtained. Thus, the three methods gave concordant results. Similar difficulties were encountered with $\text{AQS} + \text{SO}_3^{2-}$ where k_q could be reliably determined only by the competition method¹⁵ and for $\text{NQ} + \text{NO}_2^-$ where the triplet and semiquinone absorptions overlapped almost completely (around 390 nm), leaving too little of the triplet trace to be accurately determined. In this case, only the competitive method with Br^- was used, with NO_2^- kept constant.

Radical Yields. For 337-nm irradiation, quantum yields of reduced species were measured using the $\text{AQS}/2 \text{ M Cl}^-$ actinometer ($\phi_{\text{AQS}} = 0.51$).⁵ For eosin, irradiated at 480 nm, the depletion of eosin absorption (extrapolated to zero time) was used as an actinometer. Extinction coefficients ($\text{M}^{-1} \text{ cm}^{-1}$) of the anionic radical species were taken as follows:¹⁷ AQS^- , 8200 at 500 nm; NQ^- , 12 500 at 390 nm; BC^- , 7660 at 650 nm; ϵ_{max} of BS^- was assumed to be equal to that of BC^- at 650 nm; eosin, $\epsilon_{515 \text{ nm}} = 92\,000$ (for depletion measurement) and $\epsilon_{405 \text{ nm}} = 40\,000$ at λ_{max} of its radical. In the case of xanthone, ϵ_{max} (560 nm) of the reduced radical is unknown. Therefore, a xanthone solution containing 1 M SCN^- was pulsed in the absence and presence of O_2 (1 atm) (see Figure 4). The transient absorption in the O_2 -free solution gives the combined contributions of $(\text{SCN})_2^-$ and reduced xanthone at equimolar concentrations, while that produced in the O_2 -saturated solution gives (after appropriate time) only the $(\text{SCN})_2^-$ contributions. From the difference of the two spectra and the known extinction coefficients of $(\text{SCN})_2^-$ ($\epsilon_{480} = 7600$; $\epsilon_{560} = 2930$),¹⁸ $\epsilon_{560} \sim 2500$ was estimated for the reduced xanthone radical.

Corrections were made for triplet–water reactions, proceeding in competition with anion quenching. In the case of BC , BS , and NQ , this also leads to radicals contributing appreciably to the measured yield at low anion concentrations but negligibly, of course, at total quenching. Radical yields in the absence of quencher were determined separately, and their fractional con-

tributions in the presence of anions were taken to be in the ratio of quenched to unquenched triplet lifetimes. AQS triplet forms water adducts whose absorption overlaps that of the radical.¹⁶ These were determined by flashing each NO_2^- solution in the presence of O_2 , which removes the semiquinone and isolates the contaminating water–adduct absorption. With SO_3^{2-} , this method failed because O_2 is consumed by autooxidation of SO_3^{2-} , initiated by the SO_3^- radical.¹⁹ In this case, we give only limiting values of ϕ_R , measured at high SO_3^{2-} concentrations.

For irradiation at 337 nm, corrections were made for the fraction of light absorbed by NO_2^- , holding it as low as possible. Thus, in order to raise $[\text{NO}_2^-]$ up to $5 \times 10^{-2} \text{ M}$ in some AQS/NO_2^- experiments, the concentration of AQS was raised from its usual value ($2 \times 10^{-4} \text{ M}$) to $5 \times 10^{-4} \text{ M}$. This procedure was adopted after first verifying that ϕ_{AQS} , properly corrected for fractional light absorption, does not depend on $[\text{AQS}]$ in this range. (The collinear arrangement of measuring and excitation beams enabled us to raise the absorbance of the solution up to 3.5.)

Results and Discussion

Quenching Rates, Mechanisms, and Free Energy Relationships.

Table I gives new measurements of quenching rates and radical yields together with relevant rate data for various anions, taken from previous work and from the literature. Also included are the free energy changes of the charge-transfer (CT) and energy-transfer (NT) reactions of NO_2^- with the organic molecule, M . $\Delta G^\circ_{\text{CT}}$ was evaluated by means of the Rehm–Weller equation: $\Delta G^\circ_{\text{CT}} = E^\circ(\text{NO}_2/\text{NO}_2^-) - E^\circ(\text{M}/\text{M}^-) - E_T(\text{M})$, where $E^\circ(\text{NO}_2/\text{NO}_2^-)$ and $E^\circ(\text{M}/\text{M}^-)$ are the standard reduction potentials of NO_2 and the organic molecule, respectively, and $E_T(\text{M})$ is the triplet energy of M .²⁰ $\Delta G^\circ_{\text{NT}}$ is simply $E_T(\text{NO}_2^-) - E_T(\text{M})$. (For sources of data, see footnotes to Table I.)

The collected data for NO_2^- lead us to conclude that both quenching mechanisms, CT and NT, may operate for this particular anion. When both channels are endoergic ($\Delta G^\circ > 0$), the quenching becomes relatively slow ($k_q \leq 10^6 \text{ M}^{-1} \text{ s}^{-1}$). For either channel, the rate should become diffusion controlled at sufficiently exoergic conditions. The meaning of “sufficiently”, however, is not the same for the two channels. On examining those systems where *only one channel is exoergic* (grouped separately in Table I), it appears that quenching becomes dc at $\Delta G^\circ \leq -0.5 \text{ eV}$ for CT but $\Delta G^\circ \leq 0 \text{ eV}$ for NT processes. This suggests that a higher activation barrier is involved in the CT mechanism. Moreover, a comparison with other anions indicates that “pure” CT quenching by NO_2^- (Table I, second group) is slower than expected from its reduction potential. Thus, (a) eosin triplet is quenched by Γ^- somewhat faster than by NO_2^- , although the standard reduction potential of I^- (1.33 V) is considerably higher than that of $\text{NO}_2/\text{NO}_2^-$ (1.04 V),^{21,22} and (b) NO_2^- and N_3^- ($E^\circ = 1.35 \text{ V}$) quench the CT group at comparable rates. A similar anomaly is shown by SO_3^{2-} , whose E° (0.63 V at $\text{pH} \geq 7$)^{21,23} is far below that of Γ^- , although it is a less effective quencher (Tables I and II).

Quenching Rates and CTTS Energies. Another and quite direct measure of the energy required for electron detachment from an anion in solution is the CTTS spectrum.¹¹ CT quenching by anions and their CTTS transitions are essentially similar processes involving electron transfer from the anion to an acceptor, an excited neighbor molecule or solvent. Both processes occur rapidly on the nuclear time scale and therefore involve Franck–Condon strains which strongly affect both the rate constant k_q and the transition energy $h\nu$. Indeed, the inefficiency of CT quenching by NO_2^- and SO_3^{2-} relative to their redox potentials compared with Γ^- , as noted above, is reflected in their CTTS ($h\nu$) energies, which despite some uncertainties are definitely not lower than that of Γ^- .¹¹ Conversely, the CT quenching constants of NO_2^- parallel those of N_3^- , and their CTTS bands are closely located, although their redox potentials are not (Table III). Related anomalies are found in matching other $h\nu_{\text{CTTS}}$ values with equilibrium reduction potentials. Thus, we have for ClO_2^- , $E^\circ = 0.93 \text{ V}$ and $h\nu = 5.85 \text{ eV}$ (see footnote to Table III) compared with Γ^- , $E^\circ = 1.33 \text{ V}$

TABLE I: Interactions of NO₂⁻ with Organic Triplets: Quenching Rate Constants, k_q,^a Limiting Quantum Yields, Φ_R, and Energetics of Associated Charge-Transfer and Energy-Transfer Processes

M ^b	E _T (M), eV	-E°(M/M ⁻), ^c V vs NHE	ΔG° _{CT} , ^d eV	ΔG° _{NT} , ^e eV	k _q , 10 ⁹ M ⁻¹ s ⁻¹				Φ _R (max) ^o
					NO ₂	I ⁻	N ₃ ⁻	SCN ⁻	
NQ ^f	2.48	0.12	-1.32	-0.18	5.0*	8.4*	4.2*	6.0*	0.97*
AQS ^g	2.68	0.38	-1.26	-0.38	3.2	4.2	3.1	3.9	0.81*
BC ^h	2.96	1.13	-0.79	-0.66	3.0	2.3	2.1	2.2* ⁱ	0.05* ⁱ
xanthone ^j	3.21	1.40	-0.77	-0.91	5.6*	7.1*	4.9*	6.0*	0.0*
thioxanthone ^j	2.84	1.37	-0.43	-0.54	4.4*	6.6	3.8	0.03	0.0*
2-acetonaphthone ^k	2.59	1.25	-0.30	-0.29	3.2	0.014	0.0012	1.5 × 10 ⁻⁵	0.0
1-naphthaldehyde ^k	2.45	1.11	-0.30	-0.15	1.6	0.28	0.024		0.0
acetone ^k	3.40	2.1 ^l	-0.3	-1.1	3.0	7.1	0.35	2.0	0.0
1-acetonaphthone ^k	2.52	1.26	-0.22	-0.12	2.4	0.0037	2 × 10 ⁻⁴		0.0
lumiflavine ^m	2.17	0.49	-0.64	+0.13	1.5		4.3		1.0
thionine ^m	1.70	0.25	-0.41	+0.60	0.0068		0.18		>0.7
thiopyronine ^m	1.80	0.43	-0.33	+0.50	0.005		7 × 10 ⁻⁵		>0.7
eosin ⁿ	1.86	0.50	-0.32	+0.44	9 × 10 ⁻⁴ *	0.012*	0.0016*	1.2 × 10 ⁻⁵ *	~1*
fluoranthene ^k	2.30	1.77	+0.51	0.0	0.35				0
chrysene ^k	2.48	2.06	+0.62	-0.18	1.0				0
naphthalene-2-sulfonate ^k	2.65	2.34	+0.73	-0.35	2.0				0
coronene ^k	2.40	1.80	+0.44	-0.10	0.5				0
pyrene ^k	2.12	1.87	+0.79	+0.18	0.004				0

^a k_q values for other anions are included, for comparison with NO₂⁻. ^b Unless stated otherwise, sources of data for each molecule are given below. ^c These one-electron reduction potentials, in water at pH 7, may be uncertain in some cases. For a critical compilation of such potentials, see ref 21. ^d ΔG°_{CT} = E°(NO₂/NO₂⁻) - [E_T(M) + E°(M/M⁻)], with E°(NO₂/NO₂⁻) = 1.04 V.²¹ ^e ΔG°_{NT} = E_T(NO₂⁻) - E_T(M), with E_T(NO₂⁻) = 2.3 eV.^{6,7} ^f Reference 5. ^g Reference 16. ^h Reference 14. ⁱ At pH 11.2. Similar results were obtained for BS; k_q = 3.2 × 10⁹ M⁻¹ s⁻¹; Φ_R = 0.03. ^j Abdullah, K. A.; Kemp, T. J. *J. Chem. Soc., Perkin Trans. 2* **1985**, 1279. (Instead of 60% (v/v) CH₃CN used by these authors, our solutions contained 16% and 32% CH₃CN for xanthone and thioxanthone, respectively.) ^k Reference 6. ^l Schwarz, H. A.; Dodson, R. W. *J. Phys. Chem.* **1989**, *93*, 409. ^m Winter, G.; Shioyama, H.; Steiner, U. *Chem. Phys. Lett.* **1981**, *81*, 547. ⁿ E_T from: Engel, P. S.; Monroe, B. M. *Adv. Photochem.* **1971**, *8*, 245, Table XII. See also: Chambers, R. W.; Kearns, D. *Photochem. Photobiol.* **1969**, *10*, 215; Parker, C. A.; Hatchard, C. G. *Trans. Faraday Soc.* **1961**, *57*, 1894. E° from: Rao, P. S.; Hayon, E. *J. Am. Chem. Soc.* **1974**, *96*, 1280. Concordant values of k_q for I⁻ and N₃⁻ were obtained by: Kraljic, I.; Lindquist, L. *Photochem. Photobiol.* **1974**, *20*, 351. ^o Values indicated by an asterisk are from the present work.

TABLE II: Interactions of SO₃²⁻ with Organic Triplets: Quenching Rate Constants, k_q, and Limiting Radical Yields, Φ_R

M	ΔG° _{CT} , ^a V	k _q , 10 ⁹ M ⁻¹ s ⁻¹	Φ _R (max)
AQS	-1.67	2.1	0.8
BC	-1.20	0.35	0.6
xanthone	-1.18	1.1	~1
eosin Y	-0.72	0.0044	~1

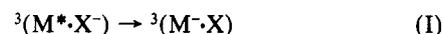
^a ΔG°_{CT} = E°(SO₃²⁻/SO₃⁻) - [E_T(M) + E°(M/M⁻)], with E°(SO₃²⁻/SO₃⁻) = 0.63 V.^{21,23} For E_T(M) and E°(M/M⁻) values, see Table I.

and hν = 5.47 eV, or HCO₂⁻, E° = 1.55 V, hν ~ 7 eV,⁵ compared with Cl⁻, E° = 2.5 V, hν = 7.1 eV. These high hν values, associated with low reduction potentials of the (X/X⁻) couple, clearly indicate large relaxation energies following photoionization or large

Franck-Condon barriers in anion oxidation.

Correlations between k_q and hν_{CTTS} values have appeared previously,^{6,24-26} but the theoretical basis for this, particularly with regard to the reorganization energy, has not been clearly recognized or discussed. An attempt in this direction, based on the classical theory of Marcus,⁸⁻¹⁰ is presented here.

Reorganization Energies from CTTS Spectra, Photoemission Thresholds, and Thermodynamic Data. Consider the case where the rate of quenching is controlled by the rate of electron transfer within the encounter pair



(M* is the excited organic molecule and X⁻ is the anion). In this case

$$k_q = \nu \exp(-\Delta G^*/RT) \quad (\text{1})$$

TABLE III: Thermodynamic, Spectroscopic, and Geometrical Properties of Inorganic Couples, X/X⁻, and Derived Reorganization Energies

anion	E°(X/X ⁻), ^a V vs NHE	hν _{CTTS} , ^b eV	E _X (sol), ^g V	E ₁ , ^h eV	R̄, eV, from				E° _{vert} , ⁱ V	r, Å		α ^o		R̄ _b (calcd), ^r eV
					CTTS ^j	E _X ^j	E _t ^k	theor ^h		X	X ⁻	X	X ⁻	
CN ⁻	~2.8	7.28	7.22		~1.9	1.92			~4.7	1.17 ^m	1.15 ⁿ			~0
Cl ⁻	2.50	7.10	7.04	8.9	1.98	1.92	1.81	4.48						0
Br ⁻	1.92	6.29	6.48	8.15	1.75	1.67	1.75	1.68	3.67					0
OH ⁻	1.91	6.59 ^c	6.65	8.6	2.06	1.80	2.21	2.18	3.97	0.97 ^m	0.97 ⁿ			0
SCN ⁻	1.66	5.73	6.52	7.2	1.45	1.07	1.06	1.67	3.11			linear ^q		~0
N ₃ ⁻	1.35	6.09 ^d	5.74	7.4	2.12	2.21	1.57	1.61	2.92 ^j	1.18 ^d	1.17 ^d	linear		~0
I ⁻	1.33	5.47	5.65	7.4	1.52	1.68	1.59	1.51	2.85					0
SH ⁻	1.15	5.40	5.57		1.63	1.69			2.78	1.34 ^m	1.34 ⁿ			0
NO ₂ ⁻	1.04	5.90 ^e	5.43	7.6	2.24	2.33	2.08	1.46	3.28	1.19 ^o	1.25 ^o	133.9 ^o	117.5 ^o	0.77
ClO ₂ ⁻	0.93	~5.85 ^f	5.70		~2.3	2.01			3.23	1.47 ^p	1.57 ^p	118 ^p	110.5 ^p	0.55

^a Reference 21. ^b Unless noted otherwise, these data were taken from papers of Fox, M. F.; Hayon, E.; and co-workers in *J. Chem. Soc., Faraday Trans. 1* as follows: CN⁻, **1990**, *86*, 257; Cl⁻, **1978**, *74*, 1776; Br⁻, **1977**, *73*, 872; SCN⁻, **1981**, *77*, 1497; I⁻, **1977**, *73*, 1003; SH⁻, **1979**, *75*, 1380. ^c Fox, M. F.; McIntyre, R.; Hayon, E. *Faraday Discuss. Chem. Soc.* **1977**, *64*, 167. ^d Burak, I.; Treinin, A. *J. Chem. Phys.* **1963**, *39*, 189. ^e Reference 35a. But see: Strickler, S. J.; Kasha, M. *J. Am. Chem. Soc.* **1963**, *85*, 2899. ^f Reference 35a. Appears as a shoulder, assignment uncertain. ^g Reference 6. ^h Reference 32. These correspond to R̄_S. ⁱ From eq 7. ^j From eq 8. ^k From eq 5. ^l E°_v = E°(X/X⁻) + R̄_{CTTS}, except for N₃⁻, for which we take R̄_t = 1.57 eV. ^m Huber, K. P.; Herzberg, G. *Molecular Spectra and Molecular Structure. IV. Constants of Diatomic Molecules*; Van Nostrand Reinhold: New York, 1979. ⁿ Del Bene, J. E.; Shavitt, I. *J. Phys. Chem.* **1990**, *94*, 5514. ^o Ervin, K. M.; Ho, J.; Lineberger, W. C. *J. Phys. Chem.* **1988**, *92*, 5405. ^p Reference 40. ^q Interatomic distances in SCN⁻ are unknown but are not likely to differ appreciably from those in SCN⁻ since electron is lost from a nonbonding orbital, as in N₃⁻. ^r Calculated using valence-bond field approximation. See text for force constants; off-diagonal terms are small.

where ν is the frequency of electron transfer within the encounter pair. The electronic barrier factor κ is included here in ν ; $\kappa \sim 1$ for adiabatic transfer. Also included is the diffusional equilibrium constant K_d for the formation of the encounter pair; its value is close to 1.²⁷ The free energy of activation, ΔG^\ddagger , can be expressed by the Marcus equation^{8,28,29}

$$\Delta G^\ddagger = \frac{\lambda}{4} \left(1 + \frac{\Delta G^\circ_{\text{CT}}}{\lambda} \right)^2 \quad (2)$$

where $\Delta G^\circ_{\text{CT}}$ is the standard free energy of the overall process (${}^3\text{M} + \text{X}^- \rightarrow \text{M}^- + \text{X}$) and λ is the total reorganization energy:

$$\lambda = \lambda_i + \frac{e^2}{2r_D} \left(\frac{1}{\epsilon_{\text{op}}} - \frac{1}{\epsilon_s} \right) + e^2 \left(\frac{1}{2r_A} - \frac{1}{r_{\text{AD}}} \right) \left(\frac{1}{\epsilon_{\text{op}}} - \frac{1}{\epsilon_s} \right) \quad (3)$$

λ_i , the *inner-sphere* reorganization energy, represents the inner contribution of the two reacting molecules together with their firmly bound solvent layers (if present), which are treated as coordinated ligands. The other terms in eq 3 represent the contribution of the polarization of remaining solvent, treated as a continuous medium with optical and static dielectric constants ϵ_{op} and ϵ_s , respectively; r_D , r_A , and r_{AD} are the effective radii of the donor (X^-), acceptor (M), and the reaction distance, respectively (see below).

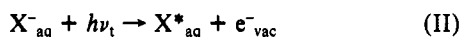
For interactions between aromatic organic triplets and simple anions, the contribution of the organic molecule to λ_i is relatively small, owing to its rigidity (no significant change in geometry on gaining an extra electron) and its loose solvation layer as compared with that of the relatively small anions. (For organic systems, it was assumed very early that λ_i can be neglected in comparison with the outer-sphere reorganization energy.²⁸)

Equation 3 then becomes

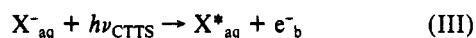
$$\lambda = \bar{R} + e^2 \left(\frac{1}{2r_A} - \frac{1}{r_{\text{AD}}} \right) \left(\frac{1}{\epsilon_{\text{op}}} - \frac{1}{\epsilon_s} \right) \quad (4)$$

where $\bar{R} = \lambda_i + (2e^2/r_D)(1/\epsilon_{\text{op}} - 1/\epsilon_s)$ is the intrinsic reorganization energy of the anion. It always contains a solvent contribution (including that of the first solvation layer) which we denote as \bar{R}_s , the energy required to organize the solvent around the radical X into the equilibrium configuration around the anion. It may also have a contribution from inner bond reorganization, denoted by \bar{R}_b . This is zero when the structures of the anion X^- and its radical are the same, as in the case of monatomic anions, and it should be relatively small for OH^- , SH^- , and the pseudohalide ions (CN^- , N_3^- , SCN^-) which suffer little change in bond lengths upon oxidation (Table III). However, if the two structures differ considerably (as for NO_2^- and ClO_2^- , Table III, or HCO_2^- , where the radical undergoes actual bond rearrangement⁵), then \bar{R}_b must be considered.

We now evaluate the overall $\bar{R} = \bar{R}_s + \bar{R}_b$ for the various anions by combining data on their CTTS spectra with the closely related spectroscopic property, the photoelectric emission threshold energy, E_i , for electron transfer from the anion in solution to vacuum.^{12,30} This latter process is



where X^*_{aq} is the Franck–Condon state of the photoionized anion. For CTTS transitions, we have



where e^-_{b} represents the electron bound in the solvent. The detailed nature of this binding is not of concern here. The energies of these processes are respectively

$$E_i = E^\circ(\text{X}/\text{X}^-) + \bar{R} + 4.48 \quad (5)$$

and

$$h\nu_{\text{CTTS}} = E^\circ(\text{X}/\text{X}^-) + \bar{R} + 4.48 - B \quad (6)$$

where $E^\circ + 4.48$ is the *absolute* standard reduction potential, E°_{Ab}

referred to the electron–vacuum level and not to the normal hydrogen electrode,^{30,31} and B is the binding energy of the electron in the solvent, relative to its vacuum level. (For remarks on approximations in these equations, see below.) In each case $E^\circ_{\text{Ab}} + \bar{R}$ is the absolute vertical redox potential of the anion.

Equation 5 offers a simple way to obtain values of \bar{R} , as has been done extensively by Delahay and co-workers.^{30,32} However, the values of E_i are subject to some ambiguity arising from the possibility of autoionization processes in polyatomic anions.^{30,33} These uncertainties do not appear in determining either E_i or $h\nu_{\text{CTTS}}$ in the case of the simple halide ions. Moreover, CTTS transitions can be assigned with some confidence in other cases, on the basis of their characteristic features (temperature and environmental effects) as exemplified in the halide spectra. We therefore prefer to base the evaluation of \bar{R} on eq 6 using the relation $B = E_i - h\nu_{\text{CTTS}}$ to obtain \bar{R} ,³⁴ with the spectroscopic parameters limited to the halides alone. The most recent values of E_i 's of Cl^- , Br^- , and I^- are respectively 8.9, 8.15, and 7.40 eV.³² Plotting these against their $h\nu_{\text{CTTS}}$ values (Table III) gives a straight line, slope = 0.92, and average $B = 1.86 \pm 0.06$ eV. The value previously derived is $B = 1.7 \pm 0.3$ eV.³⁴

Equation 6 then becomes

$$h\nu_{\text{CTTS}} = E^\circ(\text{X}/\text{X}^-) + \bar{R} + 2.62 \text{ eV} \quad (7)$$

Table III summarizes relevant data and \bar{R} values obtained both from eq 7, using recent determinations of one-electron standard redox potentials and $h\nu_{\text{CTTS}}$ values³⁵ and, for comparison, from eq 5 as well.

Another approach to \bar{R} utilizes the electron affinity of the radical X in solution, $E_{\text{X}}(\text{sol})$, defined as ΔH for the reaction



in which all species are fully equilibrated. Values of $E_{\text{X}}(\text{sol})$ for several anions, obtained from their enthalpies of formation, and an appropriate Born–Haber cycle have been given previously⁶ and are listed in Table III. To convert the products of reaction IV to $\text{X}^*_{\text{aq}} + e^-_{\text{b}}$ requires the energy input of \bar{R} and release of B . Therefore

$$h\nu_{\text{CTTS}} = E_{\text{X}}(\text{sol}) + \bar{R} - B \quad (8)$$

With $B = 1.86$ eV, eq 8 gives another set of \bar{R} 's (Table III).

Equations 5, 7, and 8 involve several approximations (but not to the same extent), including assignment of thermodynamic properties to nonequilibrium states,³⁰ neglect of entropy terms, and insufficient consideration of dielectric dispersion.³⁰ Nevertheless, in most cases the three equations yield nearly the same values of \bar{R} , indicating that the errors involved are relatively small.³⁶ It is interesting that for many anions $\bar{R} - B$ is also quite small,³⁷ so that $h\nu_{\text{CTTS}} \sim E_{\text{X}}(\text{sol})$, as has been noted previously.^{6,38}

Anion Solvation and Internal Mode Contributions to \bar{R} ; Vertical Redox Potentials. Theoretical values of the solvent contribution to \bar{R} , corresponding to \bar{R}_s , have been calculated for the anions by Delahay and Diedzic, treating interactions in the first hydration layer in detail and the remaining solvent as a continuous medium (Table III).³² These agree well ($\pm 10\%$) with the spectroscopic values, \bar{R}_{CTTS} , for those anions which undergo no appreciable change in structure in the redox reaction, i.e., with $\bar{R}_b = 0$, except for N_3^- . The reason for the high value in this case is not clear; it may reflect errors in either $h\nu_{\text{CTTS}}$ or $E^\circ(\text{N}_3/\text{N}^-)$, although the latter appears rather unlikely.²¹ Thus, a more reasonable value is obtained from the E_i data and eq 5 (see below). However, the particularly large discrepancy for NO_2^- ($\bar{R}_{\text{CTTS}} - \bar{R}_{\text{theor}} = 0.78$ eV) can clearly be associated with the considerable difference in structure between this anion and its radical (Table III). The resulting contribution, \bar{R}_b , to the reorganization energy can be estimated using a simple valence-bond field approximation: $\bar{R}_b = k_r(\Delta r)^2 + 1/2(k_\alpha/r^2)(r\Delta\alpha)^2$, where Δr and $\Delta\alpha$ are the changes in bond lengths and interbond angle, respectively, and $k_r = 9.13$ mdyne/Å and $k_\alpha/r^2 = 1.52$ mdyne/Å are the corresponding force constants in NO_2 .³⁹ The value $\bar{R}_b = 0.77$ eV thus obtained fully supports our interpretation. To complete the list of \bar{R}_b values, the same method applied to ClO_2 ($k_r = 7.23$, $k_\alpha/r^2 = 0.62$

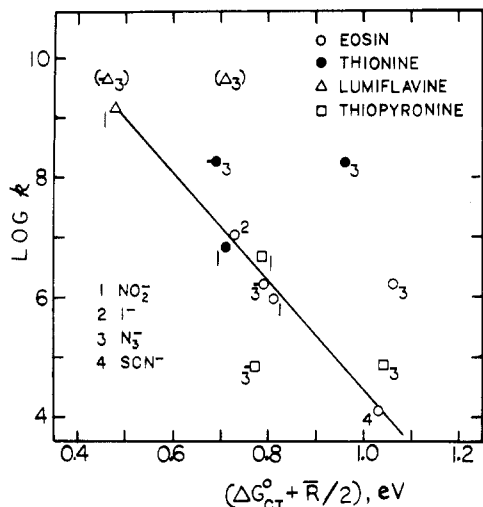


Figure 1. Dependence of rate constants, k_q , on $(\Delta G^\circ_{CT} + \bar{R}/2)$, for quenching of dye triplets by anions (Table I), using \bar{R}_{CTTS} , according to eqs 6 and 10. For N_3^- , barred points (\bar{O} ; etc.) are calculated using \bar{R}_1 , eqs 5 and 10. Two points in parentheses, for rates approaching diffusion control, are not applicable to eq 10 but are plotted to show anomalously high k_q 's for N_3^- , using \bar{R}_{CTTS} (see text).

$\text{mdyn}/\text{\AA}^{40}$ gives $\bar{R}_b = 0.55$ eV.

Vertical reduction potentials, $E_V = E^\circ + \bar{R}$, for electron transfer at nuclear configuration corresponding to the equilibrated anion are listed in Table III. These parameters should properly replace E° values in seeking correlations between $h\nu_{CTTS}$ or k_q of an anion and its redox properties. For example, E_V for the NO_2^- couple, 3.28 V, is appreciably higher than that for I^- , 2.85 V, in accord with their relative CT quenching efficiencies. Similarly, OH^- is a weaker quencher than Br^- for both triplets²⁶ and fluorescence,⁴¹ although their E° 's are nearly identical. Consideration of their E_V values (OH^- , 3.97 V; Br^- , 3.67 V) resolves this discrepancy.

Let us now assume, on the basis of the respective solvation structures of donor and acceptor, that for these M/X^- interactions the Marcus reorganization free energy can be assigned mainly to the anion. This is equivalent to taking $r_A \sim r_{AD}/2$ in eq 4 and can be justified as follows: the effective radii of the inorganic anions with their first hydration layer do not vary much around $r_D = 4.5 \pm 0.5$ \AA³² and $r_A \sim 3.6$ \AA, as recently used for the average effective radius for aromatic molecules comparable to those of Table I.²⁷ In particular, r_{AD} may be somewhat shorter than $r_A + r_D$, corresponding to the contraction ("penetration effect") of $10 \pm 5\%$ found for several self-exchange reactions in water (ref 10, Table VII). Thus, we estimate $r_{AD} \sim 7.3$ \AA $\sim 2r_A$. This leads finally to $\lambda \sim \bar{R}$, as defined in eq 4. Substituting \bar{R} for λ in eqs 1 and 2, we obtain

$$\log k_q = \log \nu - \frac{(\bar{R}/4)(1 + \Delta G^\circ_{CT}/\bar{R})^2}{2.3RT} \quad (9)$$

For $(\Delta G^\circ_{CT}/\bar{R})^2 \ll 1$, this can be reduced to

$$\log k_q = \log \nu - \frac{1}{4.6RT}(\Delta G^\circ_{CT} + \bar{R}/2) \quad (10)$$

Comparison with Experiment. Figure 1 shows the application of this relation to the second group of reactions in Table I, in which quenching by NT may be excluded and with ΔG°_{CT} calculated by the Rehm-Weller equation. The large positive deviations of the N_3^- points support our suspicion that the \bar{R}_{CTTS} value, 2.12 eV, is too high. A better fit is obtained using eq 5 with the photoemission threshold energy, $E_i = 7.4$ eV,³² giving $\bar{R}_1 = 1.57$ eV for N_3^- , which agrees also with the calculated value.³² The plotted line in Figure 1 is $\log k_q = 13.5 - 9.1(\Delta G^\circ_{CT} + \bar{R}/2)$, with slope quite close to -8.3 eV⁻¹, predicted by eq 10. With regard to the intercept, ν should range from 10^{12} to 10^{14} s⁻¹, according to Sutin, depending on whether the barrier-crossing vibration involves mainly solvent or high-frequency intramolecular modes.⁹ Evidently, changes in κ , the electronic factor, must also be con-

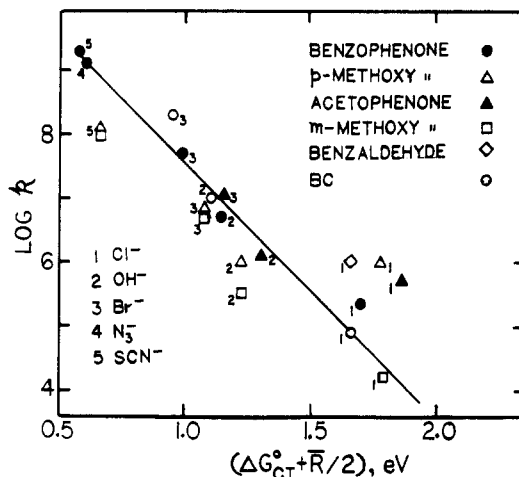


Figure 2. Dependence of rate constants, k_q , on $(\Delta G^\circ_{CT} + \bar{R}/2)$ for quenching of aryl ketone triplets by anions, according to eq 10. Data from refs 14 and 26.

sidered. On balance, the systems represented in Figure 1 appear to follow the theoretical relation, eq 10.

Less satisfactory agreement is found between eq 10 and earlier results on some carbonyl compounds.^{14,26} While the line of Figure 2, $\log k_q = 11.7 - 4.1(\Delta G^\circ_{CT} + \bar{R}/2)$, fits the data fairly well, with a reasonable value of the intercept, and the condition $(\Delta G^\circ_{CT}/\bar{R})^2 \ll 1$ still applies, the slope is half of the theoretical value. For the same values of ΔG°_{CT} , quenching of the carbonyl compounds appears to be much faster than that of the dyes shown in Figure 1; e.g., for $\Delta G^\circ_{CT} = 0$, $k_q \sim 10^8$ M⁻¹ s⁻¹, compared with 10^6 M⁻¹ s⁻¹ for the dyes. In terms of our simple model, a possible explanation is that quencher-substrate penetration associated with tight exciplex binding makes $r_{AD}/2$ smaller than r_A , thereby causing λ to become smaller than \bar{R} (eq 4). We note further that Shizuka's measurements²⁶ were made in acetonitrile-water mixtures, although our data on BC in water¹⁴ also fall close to the line of Figure 2. In any case, it seems clear that no linear correlation between $\log k_q$ and ΔG°_{CT} (assumed to be determined by correct redox potentials) can be expected without consideration of the reorganization energy.

The following relation between $\log k_q$ and $h\nu_{CTTS}$ is readily derived from eqs 7 and 10 and the Rehm-Weller expression for ΔG°_{CT} :

$$\log k_q = \log \nu - \frac{1}{4.6RT}(h\nu_{CTTS} - \bar{R}/2) + C \quad (11)$$

where

$$C = \frac{1}{4.6RT}[E^\circ(M/M^-) + E_T + 2.62]$$

Thus, for reactions between a particular acceptor, M, and various anions, $\log k_q$ should vary linearly with $(h\nu_{CTTS} - \bar{R}/2)$, provided the frequency factor, ν , remains constant. Such correlations are shown in Figure 3. Again, our very limited data for eosin (omitting N_3^-) seem to follow eq 11 with reasonable parameters. The plotted line, $\log k_q = 50 - 9(h\nu_{CTTS} - \bar{R}/2)$, compares well with the theoretical line for this case, $\log k_q = (34 + \log \nu) - 8.3(h\nu_{CTTS} - \bar{R}/2)$. Straight lines are also obtained for the systems treated in Figure 2, but their parameters are lower than expected. In general, since $\bar{R}/2$ is much smaller than $h\nu_{CTTS}$, plots of $\log k_q$ against $h\nu_{CTTS}$ should be almost linear, in contrast to $\log k_q$ vs $E^\circ(X/X^-)$, which display considerable irregularities.

Quenching by SO_3^{2-} and NO_2^- ; CT vs NT Processes. The quenching properties of SO_3^{2-} are of special interest in this study because, like NO_2^- , it behaves as a group II anion (see above) but cannot act by an NT mechanism with the triplets considered here. Rate constants for SO_3^{2-} with respect to four triplets are given in Table II. As noted above, these rates are very low, in view of the relative ease of oxidation of SO_3^{2-} ($E^\circ(\text{SO}_3^-/\text{SO}_3^{2-}) = 0.63$ V). Thus, ΔG°_{CT} values for quenching by I^- and NO_2^-

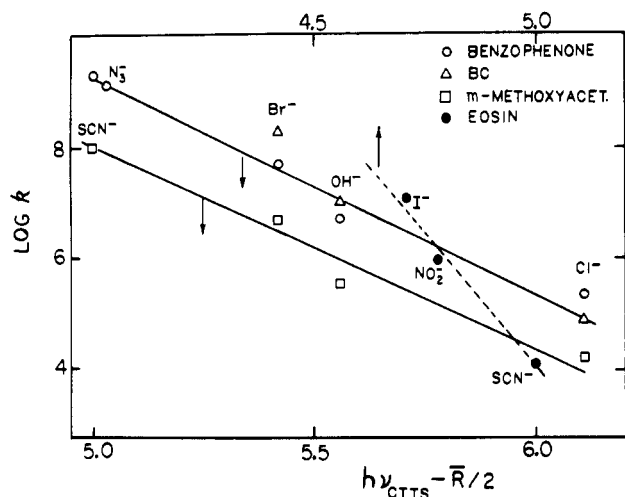


Figure 3. Dependence of rate constants for triplet quenching by anions on $(h\nu_{\text{CTTS}} - \bar{R}/2)$, according to eq 11. Lower scale (solid lines, open points) for aryl ketones; upper scale (dashed line, dark points) for eosin.

are respectively 0.7 and 0.4 V less favorable than for SO_3^{2-} , while their quenching rates are higher (except for eosin- NO_2^-) (Tables I and II). It is expected that the solvation component, \bar{R}_s , of the reorganization free energy barrier will be greater for SO_3^{2-} , in going from anionic charge two to one, than for the mononegative ions. Moreover, a contribution to \bar{R}_b is also expected. While the structure of the radical SO_3^- is not known (its interbond angle was estimated from ESR measurements to be $\sim 111^\circ$,⁴² compared to 107.1° for SO_3^{2-}), an appreciable change in shape should occur on oxidation since the electron is ejected from an orbital (6a₁) which strongly favors a decrease in bond angle.⁴² A further factor, slowing the rate with respect to charged substrates (AQS, BC, eosin), is a higher repulsive energy toward the doubly charged anion, which we have neglected in the singly charged case.²⁹ Unfortunately, attempts to evaluate \bar{R} by the methods given here are not successful. The CTTS level of SO_3^{2-} is not known, despite extensive studies,¹⁹ so that eq 7 cannot be applied. Equation 5, with $E_t = 7.2$ eV³⁰ and $E^\circ(\text{SO}_3^-/\text{SO}_3^{2-}) = 0.63$ V, gives $\bar{R} = 2.1$ eV. However, both this E_t and \bar{R} seem to be too low for a vertical ionization process. Thus, taking $E_t = 7.2$ and $B = 1.86$ eV, we obtain $h\nu_{\text{CTTS}} = 5.34$ eV, which is lower even than that of I^- , contrary to all spectroscopic evidence.¹⁹ As noted previously, Delahay pointed out the possibility of anomalously low \bar{R} values derived from photoemission at lower energies than the true E_t threshold. This will occur if the emitter undergoes autoionization from a bound-bound transition at a photon energy, $h\nu$, for which $E_X(\text{sol}) < h\nu < E_t$, where $E_X(\text{sol})$ is the equilibrium ionization potential corresponding to process IV.³⁰ Indeed, SO_3^{2-} is known to yield solvated electrons when irradiated within its internal transition band.¹⁹ However, despite these problems, the above discussion gives at least a qualitative explanation for the low quenching rates of SO_3^{2-} .

We return finally to the lower activation energy barrier for NT compared with CT, in the case of quenching by NO_2^- . This most probably originates from a lower reorganization energy, \bar{R}_s , associated with NT, simply because this process involves no change in anionic charge. With regard to \bar{R}_b , the structure of ${}^3\text{NO}_2^-$, in its lowest ${}^3\text{B}_2$ state, is closer to ground-state NO_2^- than is the case for NO_2 ; upon excitation, there is negligible change in bond length, and the ONO angle opens by $14 \pm 2^\circ$, comparable to but not greater than the change for NO_2 .⁷ Thus, assuming that the force constants in NO_2 and ${}^3\text{NO}_2^-$ are not much different, we conclude that $\bar{R}_b(\text{NT}) \lesssim \bar{R}_b(\text{CT})$.

Correlation with Thermal Self-Exchange Reactions. It is clearly of interest to correlate optically derived values of \bar{R} with those fitted to kinetic data on thermal electron-transfer reactions. Thus, Delahay and Dziedzic used \bar{R} values obtained from photoemission threshold energies to calculate free energies of activation for self-exchange reactions of some hexaquo transition-metal cations and complexes.^{30,44} The agreement with measured exchange rates

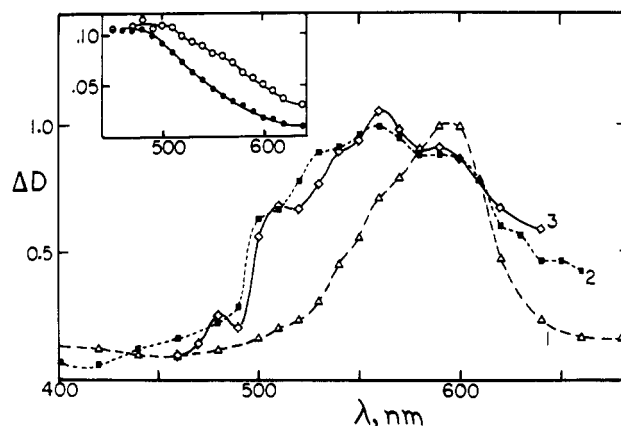


Figure 4. Transient spectra following laser photolysis of 2×10^{-4} M xanthone in 16% CH_3CN , 10^{-2} M NaOH solution. Curve 1 (dashed line, Δ): xanthone alone, N_2 -saturated, 400 ns after flash. Curve 2 (dotted line, \blacksquare): xanthone, with 0.5 M Na_2SO_3 , N_2 -saturated, 200 ns after flash. Curve 3 (solid line, \diamond): xanthone, with 1 M KSCN , difference spectrum, $D_{\text{N}_2} - D_{\text{O}_2}$ (see insert), 1 μs after flash, normalized to fit curve 2 at 600 nm. Insert: xanthone, with 1 M KSCN , saturated with N_2 (\circ) and 1 atm of O_2 (\bullet).

was quite satisfactory. However, there is little direct information on analogous reactions involving inorganic anions; most of the values for these exchange rates are indirect, based on the cross-relationships of Marcus–Hush theory.⁴⁵ For $\text{NO}_2/\text{NO}_2^-$, the rate was directly measured by Stanbury and co-workers: $k_{\text{exch}} = 580$ $\text{M}^{-1} \text{s}^{-1}$, to within a factor of 3.⁴⁶ To correlate this result with the optical value of \bar{R} for NO_2^- , we use the simplified equation derived by Delahay and Dziedzic^{30,44} for λ , the free energy of activation of the self-exchange reactions

$$\lambda = 2\bar{R} - \bar{R}_{\text{out}}$$

where $\bar{R}_{\text{out}} = e^2(\epsilon_{\text{op}}^{-1} - \epsilon_s^{-1})/2a$ and a is evaluated from the thermochemical ion radius, $a = r_{\text{ion}} + 2r_{\text{water}}$.³² This equation, which assumes equal force constants for donor and acceptor, can be readily derived from eq 3, by putting $\lambda_i = \lambda_i^{\text{D}} + \lambda_i^{\text{A}}$, $\sim 2\lambda_i^{\text{D}}$ and taking $a \sim r_{\text{D}} \sim r_{\text{A}} \sim r_{\text{AD}}/2$. With $\bar{R} = 2.24$ eV (Table III) and $\bar{R}_{\text{out}} = 0.85$ eV,³² we estimate $\lambda \sim 3.6$ eV. Using this value in eqs 1 and 2, with $\Delta G^\circ = 0$, and taking $\nu = 10^{13}$ gives $k_{\text{exch}} \sim 10^2 \text{M}^{-1} \text{s}^{-1}$. This result is much lower than the experimental value but is close to that obtained from studies using the cross-relationship, $2 \times 10^2 \text{M}^{-1} \text{s}^{-1}$.⁴⁷ On this basis, it was argued that self-exchange probably “occurs by a pathway that is more efficient than the outer sphere mechanisms implicit in Marcus theory. Presumably the transition state has substantial bonding between $\text{NO}_2(\text{aq})$ and NO_2^- .”⁴⁶ Such bonding evidently occurs for those halide and pseudohalide systems which form stable X_2^- radicals and should lead to exchange rates correspondingly faster than expected from Marcus–Hush theory.⁴⁸ The case of N_3/N_3^- is of particular interest. Applying the above procedure and taking $\bar{R} = 2.12$ or 1.57 eV (Table III) gives $k_{\text{exch}} = 4 \times 10^{-2}$ and $2 \times 10^3 \text{M}^{-1} \text{s}^{-1}$, respectively, to be compared with cross-relationship values ranging from 2×10^3 to $10^6 \text{M}^{-1} \text{s}^{-1}$.⁴⁹ These results may perhaps provide some further support for the choice of $\bar{R} = 1.57$ for N_3^- , as discussed above.

Radical Yields; Mechanism of NO_2^- -Organic Triplet Interactions. NO_2^- and SO_3^{2-} behave as typical group II anions:⁴ the yield of radicals Φ_{R} , produced by their interactions with triplets, grows almost in parallel with their quenching efficiency, $\theta_{\text{q}} = k_{\text{q}}[\text{X}^-]/(k_{\text{d}} + k_{\text{q}}[\text{X}^-])$, where k_{d} is the rate constant for triplet decay, and reaches its maximum value, $\Phi_{\text{R}}^{\text{max}}$, when quenching is practically complete. (The values of $\Phi_{\text{R}}^{\text{max}}$ are given in Tables I and II.⁵⁰) But while $\Phi_{\text{R}}^{\text{max}}$ is always high (Table II) for the SO_3^{2-} systems over a wide range of $\Delta G^\circ_{\text{CT}}$'s and k_{q} 's, this is not the case with NO_2^- . Many NO_2^- systems with high-energy triplets (e.g., BC/ NO_2^-) show little or no sign of triplet reduction despite the fact that their $\Delta G^\circ_{\text{CT}}$ is appreciably negative (Table I). Evidently, in these cases quenching by NT is indicated. Most of the given examples of this (cited in Table I) were taken from previous work,⁶

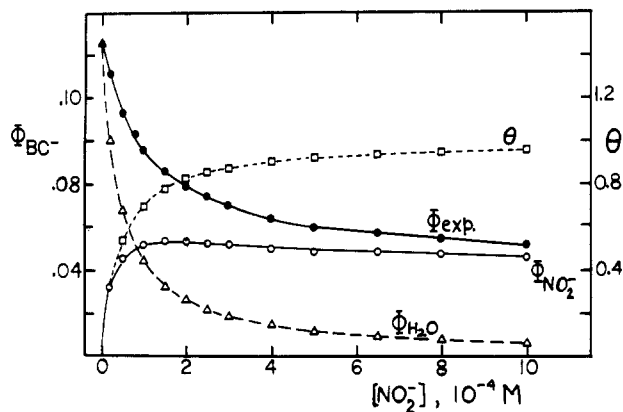


Figure 5. The BC/ NO_2^- system: effect of NO_2^- on total quantum yield of ketyl radical anion, Φ_{exp} (●). Calculated curves: quenching efficiency, θ (□); contribution of $^3\text{BC} + \text{NO}_2^-$ reaction ($\Phi_{\text{NO}_2^-}$, ○); contribution of $^3\text{BC} + \text{H}_2\text{O}$ reaction ($\Phi_{\text{H}_2\text{O}}$, △). $[\text{BC}] = 4 \times 10^{-3} \text{ M}$, pH 11.2.

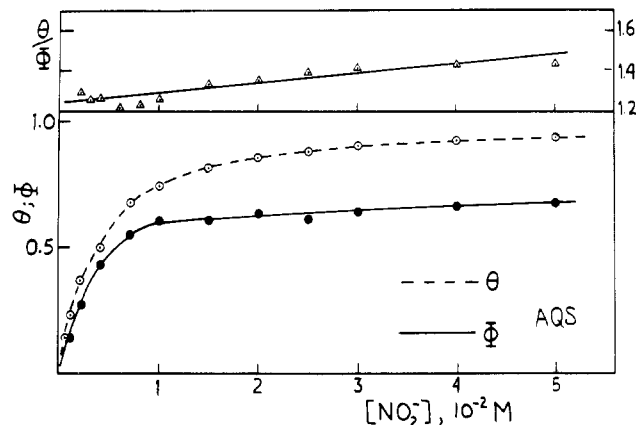


Figure 6. The AQS/ NO_2^- system: dependence of quantum yield of AQS $^-$ radical, Φ , on $[\text{NO}_2^-]$ (●). Calculated curves: quenching efficiency (○); ratio θ/Φ (insert, △). [AQS] was increased from 2×10^{-4} to $5 \times 10^{-4} \text{ M}$, to reduce fraction of light absorbed by increasing $[\text{NO}_2^-]$ (see Experimental Section).

but here we add new cases, BC, BS, xanthone, and thioxanthone. Figure 4 shows the spectra of triplet xanthone ($\lambda_{\text{max}} 595 \text{ nm}$) and its anion radical ($\lambda_{\text{max}} 560 \text{ nm}$) produced by its interaction with SO_3^{2-} in basic solution. The same radical spectrum was obtained from triplet interaction with triethylamine or with 1 M SCN^- (see Figure 4 and Experimental Section).⁵¹ On the other hand, no net chemical effect could be detected, resulting from the interaction of NO_2^- with xanthone or thioxanthone.

The case of BC/ NO_2^- (and BS/ NO_2^- which is very similar) is interesting (Figure 5). Here, addition of NO_2^- to BC actually *decreases* the yield of the radical (BC^-), and when quenching is complete, Φ_{BC^-} drops from 0.15^{52} to ~ 0.05 . This is clearly due to the greater efficiency of the triplet-water reaction to produce radicals than the competing triplet- NO_2^- reaction.

In discussing the behavior of Φ_{R} in nitrite systems, it is appropriate first to examine more closely the extent to which Φ_{R} really follows the pattern of θ_{q} . Figures 6 and 7 give results of NO_2^- quenching of AQS and NQ, respectively. The inserts show plots of $\theta_{\text{q}}/\Phi_{\text{R}}$ vs $[\text{NO}_2^-]$ which are apparently linear but not horizontal: Φ_{R} increases with $[\text{NO}_2^-]$ to a lesser extent than θ_{q} , which suggests some growing inhibition of radical production. This behavior may be explained on the basis of a mechanism previously suggested⁴ (using previous notation):

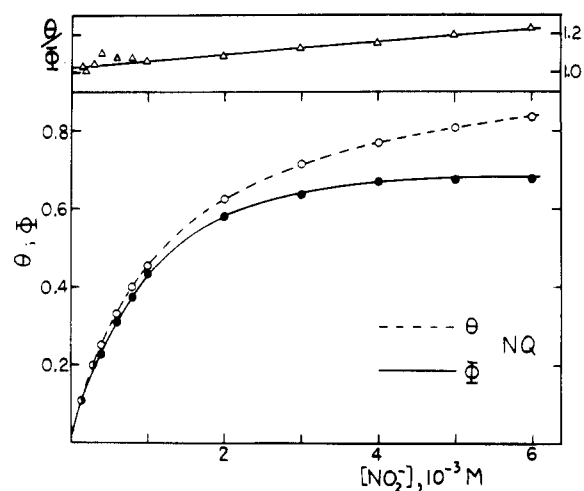
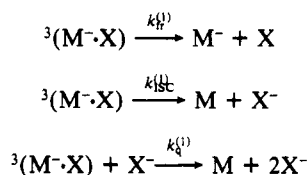


Figure 7. The NQ/ NO_2^- system: dependence of quantum yield of NQ $^-$ radical, Φ , on $[\text{NO}_2^-]$ (●). Calculated curves: quenching efficiency (○); ratio θ/Φ (insert, △). $[\text{NQ}] = 3.5 \times 10^{-4} \text{ M}$.

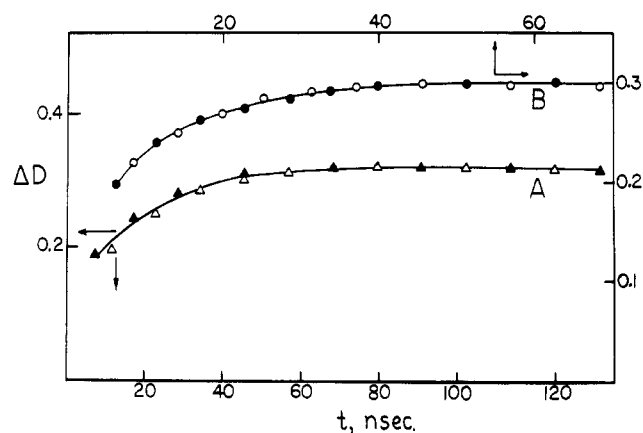


Figure 8. Kinetics of AQS $^-$ radical formation in the AQS/ NO_2^- system. Transient absorbance, ΔD_{510} vs time after flash: $[\text{NO}_2^-] = 1 \times 10^{-2} \text{ M}$ (curve A, lower time scale, △, ●) and $2 \times 10^{-2} \text{ M}$ (curve B, upper time scale, ○, ●). [AQS] = $2 \times 10^{-4} \text{ M}$ (△, ○) and $5 \times 10^{-4} \text{ M}$ (▲, ●). Absorbances are normalized to constant [AQS]. Radical growth is independent of [AQS].

in which $^3(\text{M} \cdot \text{X})$, the primary CT exciplex produced from the triplet-anion interaction with quantum efficiency θ_{q} , undergoes three parallel processes: dissociation, intersystem crossing to the ground state, and quenching by another X^- molecule. A simple kinetic analysis based on these reactions leads to

$$\theta_{\text{q}}/\Phi_{\text{R}} = (1 + k_{\text{isc}}^{(1)}/k_{\text{fr}}^{(1)}) + (k_{\text{q}}^{(1)}/k_{\text{fr}}^{(1)})[\text{X}^-] \quad (12)$$

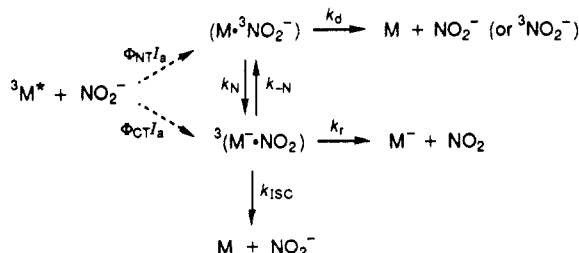
Thus, from the slopes and intercepts of the $\theta_{\text{q}}/\Phi_{\text{R}}$ vs $[\text{NO}_2^-]$ plots we derived for $k_{\text{isc}}^{(1)}/k_{\text{fr}}^{(1)}$ and $k_{\text{q}}^{(1)}/k_{\text{fr}}^{(1)}$ the following values: AQS, 0.24, 4.8 M^{-1} ; NQ, 0.03, 33 M^{-1} . We have no direct evidence for these interpretations since the proposed exciplexes have not been observed,⁵³ but the fact that they escaped detection puts an upper limit to their lifetimes, $\tau = (k_{\text{fr}}^{(1)} + k_{\text{isc}}^{(1)})^{-1} \lesssim 10 \text{ ns}$. Together with this restriction the ratios given above put a lower limit to the rate constant for exciplex quenching: $k_{\text{q}}^{(1)} \gtrsim 5 \times 10^8 \text{ M}^{-1} \text{ s}^{-1}$ for both quinones.

With regard to the drastic variation of Φ_{R} in the nitrite systems, a complication to be considered is the possibility that, when energy transfer may occur ($\Delta G_{\text{NT}}^{\circ} < 0$), it is always more efficient than CT but that triplet NO_2^- produced by NT reduces the organic molecule at a later stage if energetically permitted. The meaning of "later" is critical in considering this possibility because of the limitation imposed by the time resolution of our instruments, but we can rule out any such subsequent reduction at least at times longer than $\sim 10 \text{ ns}$. To prove this, we chose the AQS/ NO_2^- system and measured the growth rate of AQS $^-$ at relatively high $[\text{NO}_2^-]$ (10^{-2} and $2 \times 10^{-2} \text{ M}$, Figure 8) in order to determine

whether there is any lag between its fast production ($\tau = 10\text{--}20$ ns) and triplet disappearance. The total triplet decay rate was calculated by using k_d (the self-decay constant of ^3AQS) = 10^7 s $^{-1}$ ¹⁶ and $k_q^{\text{NO}_2^-} = 3 \times 10^9$ M $^{-1}$ s $^{-1}$ (Table I) as measured in dilute solutions, since at the higher concentration too little of the triplet trace was left to be accurately analyzed against the overlapping radical absorption. The radical growth rate found was actually faster by $\sim 25\%$ than the calculated triplet decay rate, which may be attributed to ionic strength effects. (At 10^{-2} M ionic strength the Brønsted equation predicts $\sim 20\%$ increase in the rate constant for a reaction between two mononegative molecules as AQS and NO_2^- .) The absence of any effect of AQS concentration on the rate constant (Figure 8) provides further evidence that no reduction of AQS occurs in bulk solution. However, this result does not exclude the possibility that the two-stage mechanism occurs at shorter times. Ultimately, this time can be so short as to blur any distinction between this mechanism and internal conversion.

In general, the results summarized in Table I support our previous conclusion³ that net reduction of triplets by NO_2^- occurs only when charge transfer is more exoergic than energy transfer. This is in keeping with the statistical theory of chemical reactions which always favors the most exoergic path.⁵⁴ In this connection, we utilize a mechanism proposed by Wilkinson¹ as a kinetic treatment of concurrent energy and charge transfer but extended here (with some simplifications) to account for radical yield.

Effect of NT on Radical Yield. Consider the following scheme, under conditions of total quenching:



The dashed arrows represent several possible intermediate stages such as formation of a common collision pair and back-reactions (see ref 1, scheme 34). The essential feature of this mechanism is the parallel formation of two distinguishable but coupled states, the NT state ($M \cdot ^3\text{NO}_2^-$) and the CT state ($^3(M \cdot \text{NO}_2)$). The overall rates of their formation are $\Phi_{\text{NT}}I_a$ and $\Phi_{\text{CT}}I_a$, respectively, where Φ signifies primary quantum yield and I_a is the intensity of light absorbed. Evidently, only the CT state yields reduced radicals M^- , with maximum quantum yield Φ_R . Steady-state treatment gives

$$\Phi_R = k_r \frac{\Phi_{\text{CT}} + \Phi_{\text{NT}}k_N/(k_N + k_d)}{k_{\text{ISC}} + k_r + k_d k_{-N}/(k_d + k_N)} \quad (13)$$

When there is no competition with energy transfer (i.e., $\Phi_{\text{NT}} = 0$, $\Phi_{\text{CT}} = 1$, and $k_{-N} = 0$), eq 13 reduces, as expected, to

$$\Phi_R = k_r/(k_r + k_{\text{ISC}}) \quad (14)$$

Another interesting case is $k_d \ll k_N$. Equation 13 then reduces to

$$\Phi_R = k_r/(k_{\text{ISC}} + k_r + k_d K) \quad (15)$$

(since $\Phi_{\text{CT}} + \Phi_{\text{NT}} = 1$). $K = k_{-N}/k_N$, the equilibrium constant of the reaction $^3(M \cdot \text{NO}_2) \rightleftharpoons (M \cdot ^3\text{NO}_2^-)$, can be related to the free energy change

$$K = \exp(\Delta G^{\circ}_{\text{CN}}/RT)$$

where $\Delta G^{\circ}_{\text{CN}} = \Delta G^{\circ}_{\text{CT}} - \Delta G^{\circ}_{\text{NT}}$ is the energy gap between the CT and NT levels. The lower is the CT level relative to the NT level, the higher is Φ_R , in agreement with our results. For $\Delta G^{\circ}_{\text{CN}} = 0$ (i.e., $\Delta G^{\circ}_{\text{CT}} = \Delta G^{\circ}_{\text{NT}}$), which is closely the case for several systems listed in Table I), $\Phi_R = k_r/(k_{\text{ISC}} + k_r + k_d)$ is determined not only by the intrinsic properties of the CT state (k_r/k_{ISC}) but

also by k_d , the deactivation constant of the NT state. However, to quantitatively test the validity of eq 15, we need more information on the kinetic properties of these postulated intermediate states.

Acknowledgment. We much appreciate support of this work by the U.S. Department of Energy, Division of Chemical Sciences, Office of Basic Energy Sciences (Grant 89ER14027, to Brandeis University), and by the U.S.–Israel Binational Science Foundation (Grant 84-00026, to the Hebrew University of Jerusalem). The Farkas Center is supported by Bundesministerium für Forschung und Technologie and the Minerva Gesellschaft für die Forschung mbH.

Registry No. NO_2^- , 14797-65-0; I^- , 20461-54-5; N_3^- , 14343-69-2; SCN^- , 302-04-5; Cl^- , 16887-00-6; OH^- , 14280-30-9; Br^- , 24959-67-9; SO_3^{2-} , 14265-45-3; PhC(O)Ph , 119-61-9; 4-OMeC₆H₄C(O)Ph, 611-94-9; AcPh, 98-86-2; AcC₆H₄-3-OMe, 586-37-8; lumiflavine, 1088-56-8; thiopyronine, 2412-14-8; eosin Y, 17372-87-1.

References and Notes

- (1) Wilkinson, F. In *Photoinduced Electron Transfer*; Fox, M. A., Chanon, M., Eds.; Elsevier: Amsterdam, 1988; p 207.
- (2) Kavarnos, G. J.; Turro, N. J. *Chem. Rev.* **1986**, *86*, 401.
- (3) Treinin, A.; Loeff, I.; Hurley, J. K.; Linschitz, H. *Chem. Phys. Lett.* **1983**, *95*, 333.
- (4) Loeff, I.; Treinin, A.; Linschitz, H. *J. Phys. Chem.* **1984**, *88*, 4931.
- (5) Loeff, I.; Goldstein, S.; Treinin, A.; Linschitz, H. *J. Phys. Chem.* **1991**, *95*, 4423.
- (6) Treinin, A.; Hayon, E. *J. Am. Chem. Soc.* **1976**, *98*, 3884.
- (7) Hochstrasser, R. M.; Marchetti, A. P. *J. Chem. Phys.* **1969**, *50*, 1727.
- (8) Marcus, R. A. *Annu. Rev. Phys. Chem.* **1964**, *15*, 155.
- (9) Sutin, N. *Acc. Chem. Res.* **1982**, *15*, 275.
- (10) Ebersson, L. *Adv. Phys. Org. Chem.* **1982**, *18*, 79.
- (11) Blandamer, M. J.; Fox, M. F. *Chem. Rev.* **1970**, *70*, 59.
- (12) Delahay, P. *Acc. Chem. Res.* **1982**, *15*, 40.
- (13) Ramsey, G. C.; Cohen, S. G. *J. Am. Chem. Soc.* **1971**, *93*, 1166. We thank Dr. Y. Naguib for this synthesis.
- (14) Hurley, J. K.; Linschitz, H.; Treinin, A. *J. Phys. Chem.* **1988**, *92*, 5151.
- (15) Sulfite shortens the lifetime of the AQS–water adduct^{4,16} until it approaches that of the triplet. This may explain the difficulty in directly measuring k_r for $^3\text{AQS-SO}_3^{2-}$.
- (16) Loeff, I.; Treinin, A.; Linschitz, H. *J. Phys. Chem.* **1983**, *87*, 2536.
- (17) For AQS, NQ^- , BC^- , and BS^- , see ref 5 and references therein. For eosin, see: Kasche, V.; Lindquist, L. *Photochem. Photobiol.* **1965**, *4*, 923.
- (18) Hug, G. L. *Natl. Stand. Ref. Data Ser. (U.S. Natl. Bur. Stand.)* **1981**, *NSRDS-NBS 69*.
- (19) Hayon, E.; Treinin, A.; Wilf, J. *J. Am. Chem. Soc.* **1972**, *94*, 47.
- (20) Rehm, D.; Weller, A. *Isr. J. Chem.* **1970**, *8*, 259.
- (21) The standard reduction potentials are taken from: Wardman, P. J. *Phys. Chem. Ref. Data* **1989**, *18*, 1637. Comparison of quenching rates on the basis of redox potentials relative to $\text{I}^-/\text{I}^\cdot$ is appropriate where the primary interaction is CT. Other factors, such as spin–orbit coupling, will be involved in controlling subsequent radical yields.³
- (22) The comparison between two anions with well-known E° also removes the uncertainty in evaluating $\Delta G^{\circ}_{\text{CT}}$, since $\Delta G^{\circ}_{\text{CT}}$ involves the one-electron reduction potential of the organic molecules which are not always reliable (see legends to Table I). The relative effects of the two anions depend only on their redox properties.
- (23) The pH values of the sulfite solutions were around 8.0.
- (24) Brooks, C. A. G.; Davis, K. M. C. *J. Chem. Soc., Perkin Trans. 2* **1972**, 1649.
- (25) Harriman, A.; Rockett, B. W. *J. Chem. Soc., Perkin Trans. 2* **1973**, 1624.
- (26) Shizuka, H.; Obuchi, H. *J. Phys. Chem.* **1982**, *86*, 1297.
- (27) Legros, B.; Vandereecken, P.; Soumillion, J. Ph. *J. Phys. Chem.* **1991**, *95*, 4752.
- (28) Marcus, R. A. *J. Chem. Phys.* **1957**, *26*, 872.
- (29) The electrostatic interaction term is neglected; it is either zero, for both reactant and product pairs for uncharged M and mononegative anion quenchers, or relatively small because of the high dielectric constant of water (see ref 10, Table 3).
- (30) Delahay, P. In *Electron Spectroscopy*; Brundle, Baker, A. D., Eds.; Academic Press: London, 1984; Vol. 5, p 123 ff. The notation corresponds to that of Delahay, with the bar added to distinguish it from the gas constant. A small correction, representing the effect of electrolyte on the surface potential, is neglected.
- (31) Noyes, R. M. *J. Am. Chem. Soc.* **1964**, *86*, 971.
- (32) Delahay, P.; Dziedzic, A. *Proc.—Indian Acad. Sci., Chem. Sci.* **1986**, *97*, 221; *Chem. Phys. Lett.* **1986**, *128*, 372.
- (33) Ballard, R. E.; Jones, J.; Hart, D. *J. Electron Spectrosc.* **1982**, *26*, 31.
- (34) Ballard, R. E.; Jones, J.; Sutherland, E.; Chun, B. L. *Chem. Phys. Lett.* **1983**, *97*, 413, 419.
- (35) (a) Friedman, H. L. *J. Chem. Phys.* **1953**, *21*, 319. (b) Throughout our discussion, $h\nu_{\text{CTTS}}$ is taken to be $h\nu_{\text{max}}$, the well-defined and accurately

measurable peak energy of the CTTS absorption band. This choice controls the value of B , and while $h\nu_{\max}$ should correspond to absorption at the most probable solvent configuration around the anion, it is still somewhat arbitrary in view of the breadth of CTTS spectra. However, it is observed that this band breadth is fairly constant for many anions.^{35a} Thus, if $h\nu_{\max}$ is used consistently in eq 6 for all the anions, and with the same value of B (eq 7), the effects on R of any uncertainty in assigning the CTTS level are minimized.

(36) If ΔS can be neglected, $E_X(\text{sol})$ is actually the absolute reduction potential. This is indicated by the expression used earlier to calculate $E_X(\text{sol})$ of organic molecules from their $E_{1/2}$: $E_X(\text{sol}) = E_{1/2} + 4.4$.¹⁶

(37) A similar conclusion can be reached from an earlier estimate that (in our notation) $\Delta H_S(\text{H}^+) + B - R_S \sim 12 \text{ eV}$.³⁵ But the value of $\Delta H_S(\text{H}^+)$, the enthalpy of solvation of H^+ , is $\sim 11.7 \text{ eV}$ (Friedman, H. L.; Krishnan, C. V. In *Water, Comprehensive Treatise*; Franks, F., Ed.; Plenum Press: 1973; Vol. 3, p 1), i.e., $B - R \sim 0.3 \text{ eV}$.

(38) Since in some cases the difference may yet be appreciable, $E_X(\text{sol})$ should not simply be replaced by $h\nu_{\text{CTTS}}$ as is done in ref 26.

(39) Herzberg, G. *Infrared and Raman Spectra*; Van Nostrand: Princeton, NJ, 1945.

(40) *Comprehensive Inorganic Chemistry*; Bailar, J. C., Emeleus, H. J., Nyholm, R., Trotman-Dickenson, Eds.; Pergamon: New York, 1972; Vol. 2, pp 1368, 1416.

(41) Shizuka, H.; Nakamura, M.; Morita, T. *J. Phys. Chem.* **1980**, *84*, 989.

(42) Atkins, P. W.; Symons, M. C. R. *The Structure of Inorganic Radicals*; Elsevier: Amsterdam, 1967; Chapter 8.

(43) Zachariassen, W. H.; Buckley, H. E. *Phys. Rev.* **1931**, *37*, 1295.

(44) Delahay, P.; Dziedzic, A. *J. Chem. Phys.* **1984**, *80*, 5793.

(45) Stanbury, D. M.; Lednický, L. A. *J. Am. Chem. Soc.* **1984**, *106*, 2847 and references therein.

(46) Stanbury, D. M.; de Maine, M. M.; Goodloe, G. *J. Am. Chem. Soc.* **1989**, *111*, 5496.

(47) Ram, M. S.; Stanbury, D. M. *J. Am. Chem. Soc.* **1984**, *106*, 8136.

(48) In this connection, see: Fairbank, M. G.; McAuley, A. *Inorg. Chem.* **1987**, *26*, 2844 and references therein.

(49) Ram, M. S.; Stanbury, D. M. *J. Phys. Chem.* **1986**, *90*, 3691.

(50) For AQS/NO_2^- and NQ/NO_2^- , Φ_R^{\max} was determined from the intercepts of the θ_a/Φ_R vs $[\text{NO}_2^-]$ plots (see text).

(51) As a typical group I anion, SCN^- reduces the triplet at concentrations which are much higher than that required for quenching.^{4,14}

(52) This value is somewhat higher than that previously reported.¹⁴

(53) The difficulty in directly determining $k_q^{\text{NO}_2^-}$ for the NQ system (see Experimental Section) may reflect interference of some overlapping absorption. This may perhaps originate from an exciplex, a possibility which should be further investigated. The lifetime of triplet NO_2^- in aqueous solution is unknown. Phosphorescence lifetimes of frozen solutions (alcoholic mixtures at 77 K) of various heavy metal nitrites have values varying from 0.25 s ($\text{Cd}(\text{NO}_2)_2$) to $\sim 5 \times 10^{-5}$ s ($\text{Pb}(\text{NO}_2)_2$ and TlNO_2) (Maria, H. J.; Armstrong, A. T.; McGlynn, S. P. *J. Chem. Phys.* **1968**, *48*, 4694). The natural lifetime of triplet NO_2^- in concentrated NaNO_2 solution, as estimated from the area of the $S_1 \rightarrow T_1$ absorption, is 0.1 s (see: Maria, H. J.; Wahlborg, A.; McGlynn, S. P. *J. Chem. Phys.* **1968**, *49*, 4925).

(54) See, e.g.: Levine, R. D.; Bernstein, R. B. *Molecular Reaction Dynamics*; Oxford University Press: London, 1974; pp 100-103, 217-221.

Bimolecular Reactions of the β -Distonic Isomer of the Ethanol Radical Cation:



Krista G. Stirk and Hilka I. Kenttämäa*

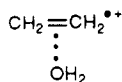
Department of Chemistry, Purdue University, West Lafayette, Indiana 47907 (Received: January 21, 1992; In Final Form: March 17, 1992)

The first experimental study on the properties of the long-lived, low-energy radical cation $^{\bullet}\text{CH}_2\text{CH}_2\text{OH}_2^+$ is reported. Bimolecular reactions of this ion and its conventional isomer, the radical cation of ethanol, have been investigated in a dual-cell Fourier transform ion cyclotron resonance mass spectrometer. Strikingly different reactivity is observed for these two radical cations. The distonic ion undergoes thermoneutral exchange of a water molecule when reacted with ^2H - or ^{18}O -labeled water. Acetonitrile readily replaces water in this ion, as well. The ethanol radical cation predominantly reacts by proton transfer with all of these reagents. The same is true for protonated ethanol. Thus, the chemical properties of the distonic ion do not reflect the ground-state structure, a covalently bound, protonated radical, which is expected to react like protonated ethanol with bases and nucleophiles. The observed reactivity is rationalized on the basis of an electrostatically bound intermediate, in accordance with the description of the distonic ion as a loosely bound ion-dipole complex of ionized ethylene and water.

Introduction

The β -distonic¹ isomer of the radical cation of ethanol, $^{\bullet}\text{CH}_2\text{CH}_2\text{OH}_2^+$, has been the subject of intensive research for over 10 years. This ion was first introduced² in 1976 by Golding and Radom, who proposed, on the basis of theoretical calculations, that certain protonated radicals may occur as intermediates in reactions catalyzed by adenosylcobalamin (a derivative of vitamin B₁₂). The ion $^{\bullet}\text{CH}_2\text{CH}_2\text{OH}_2^+$ was calculated to be about 10 kcal/mol lower in energy than the radical cation of ethanol and to have a relatively large binding energy with respect to $\text{C}_2\text{H}_4^{\bullet+}$ and H_2O (20 kcal/mol).^{2,3} These initial theoretical studies^{2,3} sparked a wide interest in this unusual isomer of ionized ethanol.

Terlouw et al.⁴ reported in 1981 the first experimental study on the ion $^{\bullet}\text{CH}_2\text{CH}_2\text{OH}_2^+$. They discovered that the fragment ion $\text{C}_2\text{H}_6\text{O}^{\bullet+}$ of 1,3-propanediol has a structure for which no stable neutral counterpart exists: the dissociation reactions of this ion are distinct from those of the two conventional isomers, $\text{CH}_3\text{CH}_2\text{OH}^{\bullet+}$ and $\text{CH}_3\text{OCH}_2^{\bullet+}$. It was proposed that this new $\text{C}_2\text{H}_6\text{O}^{\bullet+}$ ion could be represented as $^{\bullet}\text{CH}_2\text{CH}_2\text{OH}_2^+$, or as a π -bonded complex:



The heat of formation of the ion ($\Delta H_f = 175 \pm 2 \text{ kcal/mol}$) was experimentally determined in 1982 by Holmes et al.^{5a} by appearance energy measurements. A few years later, McLafferty et al. used neutralization-reionization mass spectrometry to show that ionized ethanol and its β -distonic isomer are stable toward isomerization: <3% of ionized ethanol and <0.5% of the β -distonic isomer undergo isomerization within the time scale of a sector tandem mass spectrometer when generated by 70-eV electron ionization.⁶

Further characterization⁷ of the β -distonic isomer of ionized ethanol led to the discovery of a hydrogen-bridged water-ethene radical cation complex, $\text{CH}_2=\text{CH}\cdots\text{H}^+\cdots\text{OH}_2$, on the potential energy surface. This structure was calculated⁷ to exist in a shallow potential energy well about 10 kcal/mol above the covalently bound structure $^{\bullet}\text{CH}_2\text{CH}_2\text{OH}_2^+$ and was predicted to be indistinguishable from $^{\bullet}\text{CH}_2\text{CH}_2\text{OH}_2^+$. The transition state for transfer of the water molecule between the two carbons in $^{\bullet}\text{CH}_2\text{CH}_2\text{OH}_2^+$ was calculated to be only 2-3 kcal/mol above the covalently bound structure.⁷ Because of these findings, the β -distonic ion was characterized as "a typical ion-dipole complex, with only a small contribution from sigma, pi or hydrogen bonding".⁷ Later investigators reinforced this description. McAdoo and Hudson⁸ provided experimental evidence in 1986 in support of the proposal^{2-4,7} that the water molecule can freely shift between the two